SMAP RFI CHANGE DETECTION

Priscilla N. Mohammed[1, 2], Giovanni De Amici[2], Jinzheng Peng[2, 3] and Jeffrey Piepmeier[2]

[1]Morgan State University, Baltimore, MD 21251 USA, [2]NASA's Goddard Space Flight Center, Greenbelt, MD 20771 USA, [3]Universities Space Research Association, Columbia, MD 21044 USA.

ABSTRACT

The Soil Moisture Active Passive (SMAP) mission, launched on January 31, 2015, has completed its primary 3-year mission and is currently in its extended mission. Although operation occurs within the protected frequency allocation of 1400-1427 MHz, the SMAP radiometer is impacted by radio frequency interference (RFI). The radiometer was designed to provide detection and filtering of RFI in order to meet error budget requirements. A time series algorithm was developed to monitor, detect and report the changing environment with the objective of detecting new RFI sources as well as existing persistent sources. The detection of sources are used in RFI reporting to NASA spectrum management with the hope that interfering sources will be turned off by the necessary administrations.

***Index Terms*— Microwave radiometry, radio-frequency interference (RFI)**

1. INTRODUCTION

The Soil Moisture Active Passive (SMAP) mission has been providing global measurements of soil moisture and freeze/thaw state. The SMAP radiometer operates within the 1400-1427 MHz Earth Exploration Satellite Service (EESS) passive frequency allocation, however, radio frequency interference (RFI) has plagued measurements at this frequency [1], [2]. In response to the RFI troubled environment at L-band, the SMAP radiometer hardware was designed to produce science products to enable multiple detection algorithms in ground processing [3], [4], [5], and [6].

The radiometer outputs data for computation of the full Stokes vector as well as the kurtosis for both vertical and horizontal polarizations. Two independent streams of data are produced – one over the full bandwidth and another over 16 x 1.5-MHz subband channels. The RFI detection methods implemented on both streams of data include kurtosis detection and polarimetric detection using the third and fourth Stokes parameters. Pulse detection is implemented on the fullband data while cross-frequency detection is implemented on subband data. The RFI flags from the detection algorithms are combined with a logical OR, corrupted pixels in the time/frequency footprint are dropped and remaining pixels are averaged. On orbit data show that the RFI detection algorithms are working well to detect and filter RFI to improve the quality of the SMAP brightness temperature measurements. However, some areas of the globe remain problematic as RFI that is very high level and persistent results in high percentages of data loss due to removal of bad data. Furthermore, in some instances, there are RFI sources that go undetected by the algorithm [7].

To address the challenge of RFI at L-band, a new time series algorithm was developed to detect new RFI sources appearing since launch as well as to monitor existing sources to date. Detection of high level, persistent sources identified by the change detection algorithm have been reported to NASA spectrum management using ITU interference reports (ITU-R RS.2106-0). These reports have been forwarded to administrations of countries identified with RFI sources with the hope that interfering sources will be investigated and turned off. While RFI detection and filtering has become a necessity, strong protection of the passive use of the spectrum has proven to be imperative as well.

2. CHANGE DETECTION

A time series monitor can potentially reveal new sources or problematic sources that are not detected by current processes. The new algorithm approach is as follows. The globe is divided into 0.2-degree bins and data are posted to 0.4-degree bins. Statistics are calculated over an 8-day orbit cycle for each 0.2-degree bin. Included in the statistics are the mean, standard deviation, as well as minimum and maximum values of antenna temperature, NEDT (Noise Equivalent Delta Temperature) and RFI intensity. (RFI intensity is the difference of the antenna temperature before and after RFI filtering.) The antenna temperatures and NEDT values are reported in the L1B_TB product and their statistics were computed from September 2015 to October 2018.

The process searches for deviations of RFI intensity outside expected norms. The norms, reference mean and standard deviation are computed using data from the first 6 months. Subsequent data are then used to search for significant deviation of behavior using the formalism of the Shewart control chart [8]. For each 0.2-degree bin, the difference of the average RFI intensity and the reference mean is divided by the reference standard deviation and the results are used to monitor RFI change. Figure 1 shows an example of this process, which can be used to detect change in RFI. Using the control charting method described above, an RFI source detected over Italy does not appear until almost 3 years after launch. The method can also be used to determine if sources are turned off as well.

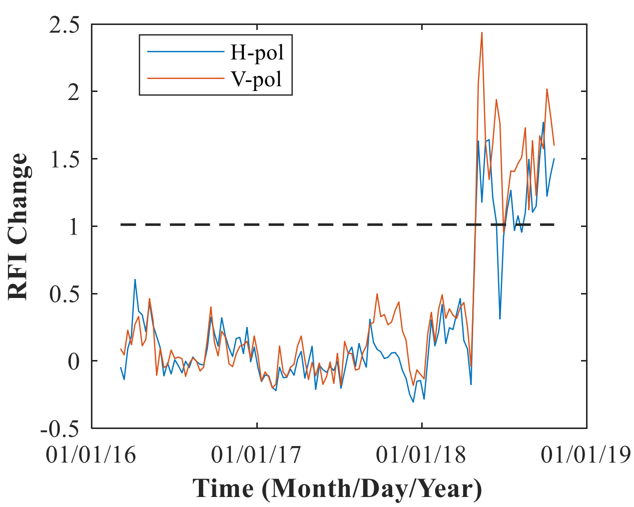

Figure 1. Control charting method used to detect RFI change. A new source over Italy appeared 3 years after launch.

3. CHANGE VECTOR

Global observations indicate a decreasing trend in RFI over China and several transient sources turning on and off globally since launch. The process of control charting using RFI intensity works well for low level RFI; however, low level RFI is transient. The algorithm may blank whole footprints with high level RFI. As a result, RFI intensity cannot be calculated for high level RFI and the time change algorithm will miss the detection. However, additional information is available. The radiometer L1B_TB product contains a quality flag, which indicates the quality of brightness temperatures based on various conditions [9].

Statistics from bit 15 of the L1B_TB quality flag was coupled with RFI intensity to create a change vector. Bit 15 is set if the brightness temperature is out of range (> 330 Kelvin), all pixels or all but one pixel remains in the footprint, the NEDT is greater than 2 Kelvin or the RFI intensity is greater than 100 Kelvin. If the flag is set, the user is advised that the data quality is not good.

For each 0.2-degree bin, the percentage of data flagged by bit 15 was calculated for each 8-day orbit cycle. When added to the change vector, the change in high level RFI was captured. Figure 2 shows global results of data flagged by bit 15. The figure shows the percentage of time 25 % or more of data within a pixel is flagged for six consecutive weeks in September and October of 2018. These sources revealed by bit 15 are candidates for RFI reporting and enforcement as high level RFI are easier to detect on the ground.

4. RESULTS

The L-band Soil Moisture Ocean Salinity (SMOS) mission has been alerting national spectrum management authorities, including China, about RFI sources, resulting in the elimination of many interfering transmissions [10]. In keeping with preserving spectrum, SMAP data are being used to create RFI reports with hope of a similar outcome. These reports are forwarded to necessary authorities via the NASA spectrum office. A SMAP RFI report was filed for sources detected in China in December 2016, which included 240 geolocated sources. Figure 3 shows the time series of the average percentage of footprints flagged by bit 15 for the sources reported in China.

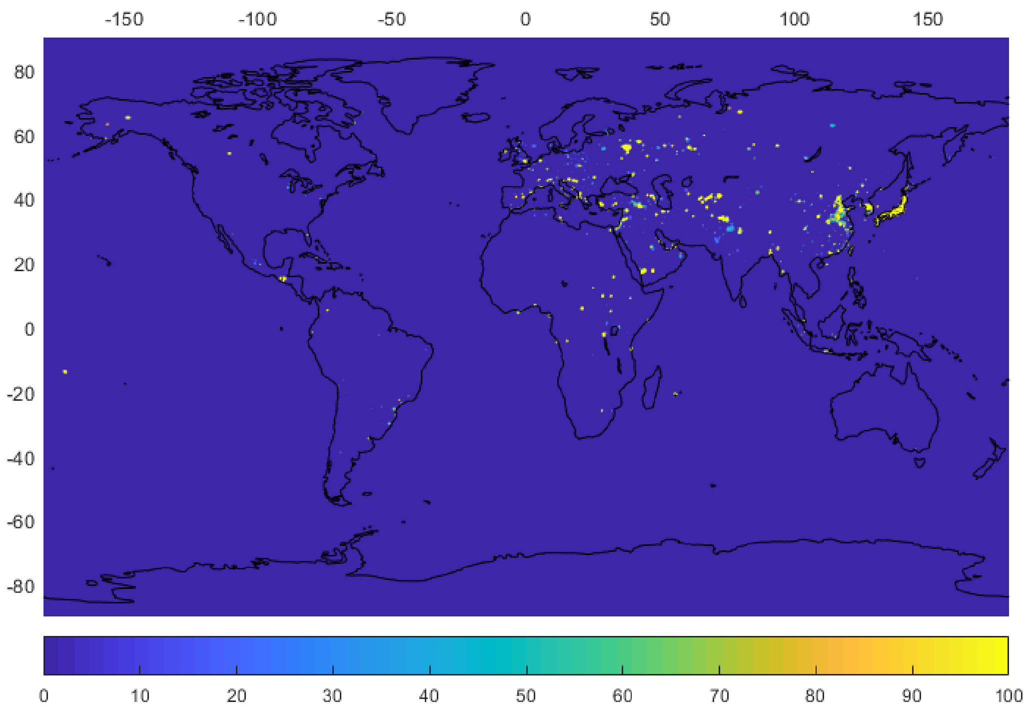

Figure 2. Horizontal polarization of data flagged using bit 15. Percentage of time bit 15 flags 25 % or more data in each pixel for six consecutive weeks in September and October of 2018.

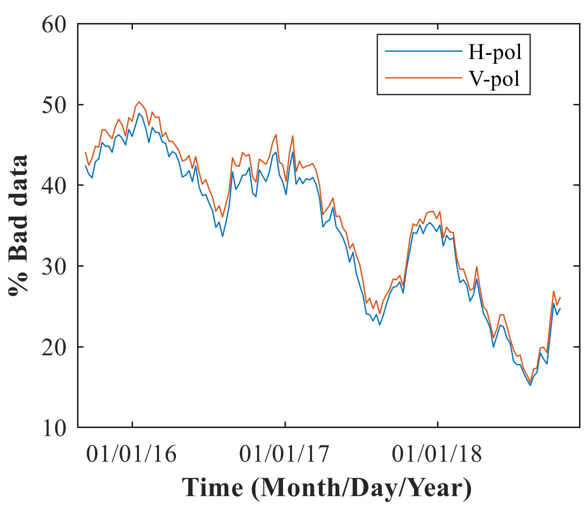

Figure 3. Time series of the average percentage of footprints flagged by bit 15 for the RFI sources reported over China.

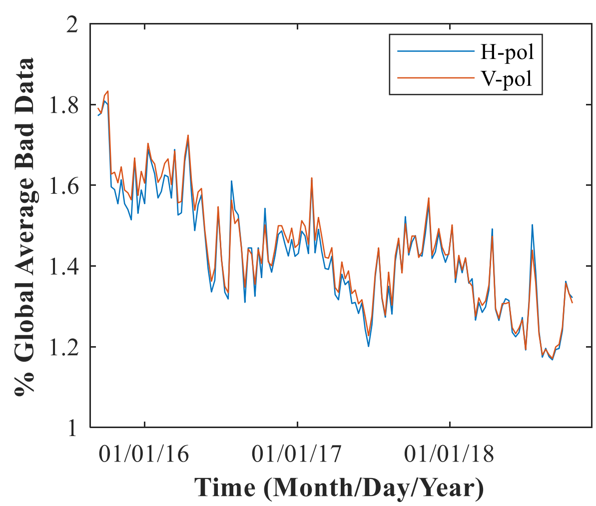

Figure 4. Time series of the average percentage of footprints flagged by bit 15 globally over land.

Figure 3 shows a decreasing trend of RFI over China, although significant RFI remains. It is uncertain whether the RFI reporting influenced this trend. It is interesting to note the cyclic pattern of RFI over this region in addition to the downward trend; however, the reasons for the trends have not been identified. Figure 4 is the time series of the average percentage of RFI that was flagged by bit 15 globally over land. While RFI remains globally, a downward trend is also observed.

The results to be presented will show that both the RFI intensity and bit 15 values in the change vector indicate a downward trend of RFI over China. The change vector was used to monitor sources turning on and off after launch. Global results indicate transient RFI sources occur over the world while persistent, high level sources are mostly concentrated in Europe and Asia. The results of this work will be used to improve the RFI reporting process and can be used to monitor regions where RFI reports were filed.

6. REFERENCES

[1] R. Oliva, E. Daganzo, Y. H. Kerr, S. Mecklenburg, S. Nieto, P. Richaume, and C. Gruhier, “SMOS RFI scenario: Status and actions taken to improve the RFI environment in the 1400-1427 MHz passive band,” *IEEE Trans. Geosci. Remote Sens*., vol. 50, no. 5, pp. 1427–1440, May 2012.

[2] S. Misra and C. S. Ruf, “Detection of radio frequency interference for the Aquarius radiometer,” IEEE Trans. Geosci. Remote Sens., vol. 46, no. 10, pp. 3123–3128, Oct. 2008.

[3] J. R. Piepmeier, J. T. Johnson, P. N. Mohammed, D. Bradley, C. Ruf, M. Aksoy, R. Garcia, D. Hudson, L. Miles, and M. Wong, “Radio-Frequency Interference Mitigation for the Soil Moisture Active Passive Microwave Radiometer,” *IEEE Trans. Geosci. Remote Sens.*, vol. 42, no. 1, pp. 761-775, Jan. 2014.

[4] C. S. Ruf, S. M. Gross, and S. Misra, “RFI detection and mitigation for microwave radiometry with an agile digital detector,” *IEEE Trans. Geosci. Remote Sens*., vol. 44, no. 3, pp. 694–706, Mar. 2006.

[5] N. Niamsuwan, J. T. Johnson, and S. W. Ellingson, “Examination of a simple pulse blanking technique for RFI mitigation,” Radio Sci., vol. 40, no. 5, pp. RS5S03-1–RS5S03-5, Oct. 2005.

[6] Balling, J. E., S. S. Sobjaerg, S. S. Kristensen, N. Skou, “RFI detected by kurtosis and polarimetry: Performance comparison based on airborne campaign data,” 12th Specialist Meeting on Microwave Radiometry and Remote Sensing of the Environment (MicroRad) 2012, Rome, Italy, March 2012. **DOI:** 10.1109/MicroRad.2012.6185255

[7] P. N. Mohammed, M. Aksoy, J. R. Piepmeier, J. T Johnson and A. Bringer, “SMAP L-Band Microwave Radiometer: RFI Mitigation Prelanch Analysis and First Year On-Orbit Observations”, *IEEE Trans. Geosci. Remote Sens.*, vol. 54, no. 10, pp. 6035–6047, October 2016.

[8] D.J. Wheeler, *Understanding statistical process control.* Knoxville: SPC Press, 2012.

[9] P. Mohammed-Tano, “Soil Moisture Active Passive (SMAP) project level 1B-TB product specification document. Pasadena, CA. USA: SMAP Project,” Jet Propulsion Lab., Pasadena, CA, USA, JPL D-92339, 2015.

[10] E. Daganzo-Eusebio, R. Oliva, and Y. H. Kerr, “SMOS radiometer in the 1400–1427 MHz passive band: Impact of the RFI environment and approach to its mitigation and cancellation,” *Trans. IEEE Geosci. Remote Sens.* vol. 51, no. 10, pp. 4999–5007, Oct. 2003.